

Neutron pickup by alpha particles to unbound states*

D. R. Brown,[†] I. Halpern, J. R. Calarco,[‡] and P. A. Russo[§]

Nuclear Physics Laboratory, University of Washington, Seattle, Washington 98195

D. L. Hendrie and H. Homeyer^{||}

Lawrence Berkeley Laboratory, Berkeley, California 94720

(Received 26 April 1976)

Two conspicuous peaks are observed in the two-dimensional coincidence spectra of α particles and neutrons emitted in bombardments of ^{12}C , Rh, ^{208}Pb , and U with 90 MeV α particles. Through their energy-angle correlation these peaks are identified as arising from the breakup products of ^5He (g.s.) formed in the (α , ^5He (g.s.)) reaction. A somewhat less prominent peaking of events is identified as the signature for the breakup of $^6\text{He}^*(1.8\text{ MeV})$ formed by two-neutron pickup. A distorted-wave Born-approximation calculation was carried out for the (α , ^5He (g.s.)) reaction on ^{208}Pb and was found to fit the measurements. The large differential cross section for the (α , ^5He (g.s.)) reaction confirms an earlier interpretation of the somewhat square structure observed in the spectra of inelastically scattered α particles.

NUCLEAR REACTIONS ^{208}Pb , Rh, ^{12}C , $^{\text{nat}}\text{U}(\alpha, ^5\text{He})(\alpha, ^6\text{He}(1.8\text{ MeV}))$, $E=42, 90$ MeV, measured two-dim α -n coin. Spectra, deduced $\sigma(\theta)$ for $^{208}\text{Pb}(\alpha, ^5\text{He})$, compared DWBA.

I. INTRODUCTION

In studies of broad range inelastic α particle spectra from heavy elements with incident beams up to 90 MeV, Chenevert *et al.* observed¹ some structure in the α' spectra which strongly suggested that some of the observed α particles were products of the decay of ^5He in its ground state (g.s.) formed in the (α , ^5He (g.s.)) reaction. In particular, they saw a square bump, or *mesa*, in the inelastic spectrum whose character appeared to match the kinematic requirement for this reaction. The implied cross section for ^5He production was large (~ 30 mb) and we therefore decided to confirm it by direct observation of the α -n coincidences from the breakup of the ^5He (g.s.), and at the same time to examine some of the basic features of this pickup reaction.

Studies in which the *target nucleus* is left in some unbound state are fairly common.^{2,3} Even though one would expect that the complementary situation (where the projectile or its direct descendant is left in an unbound state) is about equally likely to occur, there have been relatively few studies of such reactions. The main reasons for this lack of attention are the complexities of detecting particles which break apart before reaching a detector.

Reactions which lead to unbound states differ in no essential way from those that lead to bound states. At moderate bombarding energies one must consequently expect most direct reactions to populate unbound residual states rather sub-

stantially. The expected large cross sections for such reactions makes it interesting to understand their systematics and their connections with other reactions. Unbound states of the lighter partner may generally be even more interesting than those of the heavy partner because their lifetimes can be very short. Whereas unbound states in heavier nuclei tend to live for thousands of nuclear crossing times, lifetimes of such states in light nuclei can be comparable to projectile passing times. There must therefore be some sort of continuum between reactions which are best described in the ordinary way, but where the outgoing particle happens to be unbound, and reactions where three final particles begin to separate while still in each other's force fields. Among the motivations for the present coincidence study and others like it is the improvement of our understanding of these reactions. Simple reactions of this kind which have been studied before, especially at lower incident energies, involve the breakup of outgoing excited deuterons,⁴ unstable ^8Be (g.s.),⁵ and other light particles.⁶

We thus set out to study correlated α -n coincidences in α particle bombardments somewhat generally and to watch for evidence for ^5He (g.s.) production more particularly. It was decided to study ^5He production rather than the easier to detect ^5Li production because theoretical estimates and a preliminary search showed that the production cross section for the Li is several orders of magnitude less than that for the He in heavy nuclei.⁷

The most striking features in the α -n coincidence

spectra and angular correlations are indeed associated with the production of ${}^5\text{He}$ (g.s.). The characteristic kinematical features of this production are reviewed in Sec. II and the experimental details of the measurements are outlined in Sec. III. The results are described in Sec. IV in three separate parts. The first gives the evidences for the $(\alpha, {}^5\text{He}(\text{g.s.}))$ reaction, the second discusses some of the findings about this reaction, and the last tells about correlated α - n events that are not connected with ${}^5\text{He}(\text{g.s.})$ production. In the following section, Sec. V, we review some of the recent theoretical studies of the $(\alpha, {}^5\text{He}(\text{g.s.}))$ reaction and describe the results of calculations of our own with a full-recoil finite-range distorted-wave Born-approximation (DWBA) code. The paper concludes with a brief summary of results and questions raised by this work. Somewhat less extensive accounts of the $(\alpha, {}^5\text{He}(\text{g.s.}))$ reaction have been given earlier.^{8,9}

II. BREAKUP KINEMATICS

The correlations in energy and angle between the neutron and α particle from the ${}^5\text{He}$ ground state are very distinctive and serve to distinguish events which proceed through that state from the numerous other α - n coincidence events which one observes. Because of its importance in both the design and interpretation of the experiment, it is useful to review, at this point, some of the main features of the ${}^5\text{He}$ breakup kinematics. For this purpose we consider a ${}^5\text{He}$ nucleus with internal energy E_c moving along in free space with kinetic energy E_5 . The ${}^5\text{He}$ decays in flight into a neutron and an α particle whose kinetic energies in their c.m. system sum to E_c . The relevant momenta for a typical breakup are illustrated in Fig. 1.

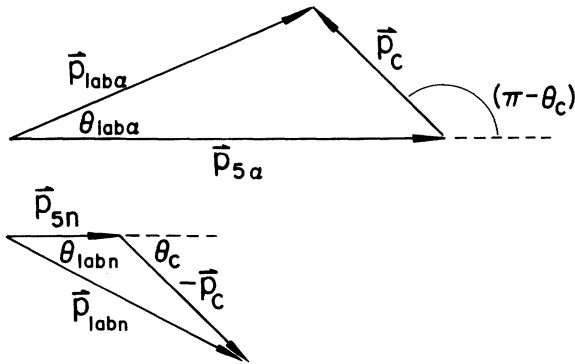


FIG. 1. The relevant momenta in the breakup of ${}^5\text{He}$. The α particle's laboratory momentum $\vec{P}_{\text{lab}\alpha}$ is the resultant of its share $\vec{P}_{5\alpha}$ of the momentum of the ${}^5\text{He}$ particle and of \vec{P}_c the momentum it picks up from the internal energy of the ${}^5\text{He}$. The lower triangle gives the corresponding momenta for the neutron.

In this figure $\vec{P}_{5\alpha}$ stands for the α particle's share of the ${}^5\text{He}$ momentum. It is four times the neutron's share, \vec{P}_{5n} . The momenta in the c.m. system of α particle and neutron are equal and opposite, of magnitude $|\vec{P}_c| = (\frac{2}{5}mE_c)^{1/2}$, where m is the nucleon mass. The momenta due to the ${}^5\text{He}$'s motion have magnitudes $|\vec{P}_{5\alpha}| = (\frac{32}{5}mE_5)^{1/2}$ and $|\vec{P}_{5n}| = (\frac{2}{5}mE_5)^{1/2}$ for α particle and neutron, respectively.

Maximum opening angles: Because $|\vec{P}_c|$ is rather small in these measurements compared with the momenta associated with the ${}^5\text{He}$ motion, both α particle and neutron emerge in the laboratory at fairly small angles to the ${}^5\text{He}$ flight direction. In particular,

$$\begin{aligned} \theta_{\text{lab}\alpha}^{\text{max}} &= \sin^{-1}(|\vec{P}_c|/|\vec{P}_{5\alpha}|) = \sin^{-1}[\frac{1}{2}(E_c/E_5)^{1/2}] \\ &\approx \frac{1}{2}(E_c/E_5)^{1/2} \end{aligned} \quad (1a)$$

and

$$\begin{aligned} \theta_{\text{labn}}^{\text{max}} &= \sin^{-1}\left(\frac{|\vec{P}_c|}{|\vec{P}_{5n}|}\right) = \sin^{-1}[2(E_c/E_5)^{1/2}] \\ &\approx 2(E_c/E_5)^{1/2}. \end{aligned} \quad (1b)$$

At incident α particle energies of 90 MeV, for example (where most of our work was done), the energy E_c is only about 1% of typical values for E_5 , and the α particle is therefore emitted within 3° of the original ${}^5\text{He}$ flight direction, and the neutron is emitted within an angle which is 4 times as large.

Laboratory energies of the breakup products: It is easy to appreciate from Fig. 1 that the expression

$$E_{\text{lab}\alpha}^{(\text{max})} = \frac{1}{8m}(|\vec{P}_c \pm \vec{P}_{5\alpha}|^2)$$

gives the maximum (plus sign) and minimum (minus sign) laboratory energies of the α particle. These are easily shown to be

$$E_{\text{lab}\alpha}^{(\text{max})} = \frac{4}{5}E_5[1 \pm \frac{1}{2}(E_c/E_5)^{1/2}]^2. \quad (2a)$$

Similarly,

$$E_{\text{labn}}^{(\text{max})} = \frac{1}{5}E_5[1 \pm 2(E_c/E_5)^{1/2}]^2. \quad (2b)$$

These extremum energies occur when the breakup direction happens to be in line with the ${}^5\text{He}$ flight direction and $E_{\text{lab}\alpha}(\text{max})$ occurs together with $E_{\text{labn}}(\text{min})$, and $E_{\text{lab}\alpha}(\text{min})$ occurs with $E_{\text{labn}}(\text{max})$. It will be of interest to know the ratio of the maximum to the minimum α particle and neutron energies. From Eqs. (2)

$$\frac{E_{\text{lab}\alpha}(\text{max})}{E_{\text{lab}\alpha}(\text{min})} = \left[\frac{1 + \frac{1}{2}(E_c/E_5)^{1/2}}{1 - \frac{1}{2}(E_c/E_5)^{1/2}} \right]^2 \approx 1 + 2(E_c/E_5)^{1/2} \quad (3a)$$

and

$$\frac{E_{1abn}(\max)}{E_{1abn}(\min)} = \left[\frac{1 + 2(E_c/E_5)^{1/2}}{1 - 2(E_c/E_5)^{1/2}} \right]^2. \quad (3b)$$

The α particle (or neutron) breakup spectrum in the laboratory takes on a very simple form for breakups that are isotropic in the c.m. system. Since $P_{1ab}^2 = P_5^2 + P_c^2 + 2P_5P_c \cos\theta_c$, it follows from the isotropy assumption, $dN/d(\cos\theta_c) = \text{const}$, that $dN/dP_{1ab}^2 = \text{const}$ or that the laboratory energy distribution dN/dE_{1ab} is a constant extending from $E_{1ab}(\min)$ to $E_{1ab}(\max)$. It was the observation of a square bump of this sort in the α, α' spectra which were observed¹⁰ with 90 MeV α particles that first suggested the production and subsequent decay of ^5He particles.

Ratio of counting rates for forward to backward breakup: One of the most distinctive features of the ^5He (g.s.) breakup is the coincidence spectrum observed when neutron and α particle counters are coaligned, i.e., when the breakup occurs along the ^5He flight direction. Then, as we have seen, the coincident α particle energies will be $E_{1ab\alpha}(\max)$ and $E_{1ab\alpha}(\min)$ exclusively with corresponding values for the neutron energies. It is of interest to know the relative rates of entry into the detectors for the two groups in the coincidence spectrum; i.e., it is useful to know the relative geometrical efficiencies. Now the ratio of solid angles in the forward direction for center of mass and laboratory systems, $d\Omega_c/d\Omega_{1ab}$, is simply P_{1ab}^2/P_c^2 . The chance that an α particle will be detected is proportional to this quantity. Thus the ratio of detection probabilities for α particles which are emitted forward and backward in the c.m. system is simply $E_{1ab\alpha}^F/E_{1ab\alpha}^B$. (We are making use here of the equality of fore and aft emissions in the c.m. system, i.e., of the parity conservation of nuclear forces.) In order to obtain the full geometric efficiencies, the α particle detection efficiencies must be multiplied by the chances to detect the coincident neutrons. The factor associated with the neutrons is, of course, the same as that for the α particles. The overall ratio of geometric efficiency for forward α 's (backward n 's) to backward α 's (forward n 's) is therefore

$$\eta(F/B) = \frac{E_{1ab\alpha}^F E_{1abn}^B}{E_{1ab\alpha}^B E_{1abn}^F}. \quad (4)$$

Making use of Eqs. (3) and the value $(E_c/E_5)^{1/2} = 0.1$ which is about right for 90 MeV α particles, we find that $\eta(F/B) \approx \frac{1}{2}$, that is, only about half as many coincident pairs strike the detectors when the α particle is the forward partner in the c.m. system compared with the number when it is the

neutron which is forward.

The foregoing discussion of the ^5He breakup kinematics is, of course, an idealization. We have not considered effects due to the distributions in E_5 (arising from the spread in residual excitations in the struck nucleus) nor in E_c (arising from the finite width of the ^5He ground state). Nor have we considered effects of the nuclear Coulomb field on the breakup trajectories. These higher order effects will be considered separately. They give rise to some blurring of the simple relations we have been examining.

III. EXPERIMENTAL DETAILS

When it was decided to do an α - n coincidence study to see whether the mesa seen in the (α, α') spectra arises from ^5He production, we naturally thought of looking for evidence for ^5Li production as well. It is, of course, easier to study coincidences between particles both of which are charged, but one must expect Coulomb suppression of ^5Li production relative to ^5He production in heavy nuclei. A crude DWBA calculation suggested, in fact, that at 42 MeV the $^5\text{Li}/^5\text{He}$ production ratio should be about 1%.⁷ An early measurement showed that the ^5Li production cross section was no more than 0.1% of that needed to account for the size of the observed (α, α') mesa. Although relatively more ^5Li are produced at 90 MeV than at 42 MeV, they are still rather few. It seemed most reasonable to begin these studies by a measurement of the much larger cross section, that for the production of ^5He .

The energies of the incident α particle were chosen to be 42 and 90 MeV, the first being the energy of the University of Washington cyclotron and the latter being an energy at which the (α, α') mesa had been clearly seen in runs at the Berkeley 88-in. cyclotron. Most of the data were taken (once again at Berkeley) at the higher incident energy. One advantage of running at the higher energy is that it raises the energies of the coincident neutrons. The minimum energy of these neutrons, according to Eq. (2b), is $0.2E_5[1 - 2(E_c/E_5)^{1/2}]^2$. At 42 MeV, the ^5He kinetic energy E_5 associated with the production of low residual excitations (these are the most probable) is about 35 MeV. At 90 MeV, the corresponding value of E_5 is about 83 MeV. The implied minimum neutron energies are ~ 3.5 and ~ 10 MeV, respectively. Since the first of these energies is close to that of evaporated neutrons whereas the second is well above this energy, it is much easier, at the higher bombarding energy, to discriminate against the many events where an inelastically scattered α particle is followed by the evaporation of a neutron. More-

over, the efficiencies of neutron detectors typically vary much more slowly with neutron energy at 10 MeV than they do at energies much closer to the detector threshold.

The main target used in these studies was a 12 mg/cm² ²⁰⁸Pb target, an isotope that Chenevert had studied.¹⁰ To explore the importance of the pickup reactions at additional locations in the Periodic Table, some runs were also carried out with ¹²C (1 mg/cm²), ¹⁰³Rh (10 mg/cm²), and ^{nat}U (47 mg/cm²).

Most of the runs with ²⁰⁸Pb were taken with the α particle counter at 22° [recall (Sec. II) that at 90 MeV, the α particle direction is, within 3°, the same as the direction of the ⁵He from which it comes]. With the α counter held at 22° the neutron counter was placed at a number of angles, some within the kinematically allowed ⁵He breakup cone and some outside it. A run with ²⁰⁸Pb was also taken with the α counter at 27° in order to see how the ⁵He differential cross section was changing with angle. The other three targets were studied with the angle of the α counter restricted to 22°.

The α detector was a two-counter solid state telescope that provided signals for particle identification and the α particle energy. The neutron detector was a 5 cm × 5 cm cylinder of NE 213 organic liquid scintillator viewed by a standard photomultiplier tube. Photon pulses in this detector were eliminated by a pulse shape discrimination circuit, and fast timing with respect to the α particle was used to measure the energy of coincident neutrons with pulse heights above a threshold value.

To maintain adequate counting rates the counters were placed at such distances that they typically subtended 5° at the target. This angular resolution was adequate in view of the various effects which smear the angular patterns of the idealized kinematics discussed in Sec. II. For example, according to Eq. (1b), the spread in the maximum angle at which the neutron is emitted that arises from the finite width Γ of the ⁵He ground state is $\Gamma/(E_c E_s)^{1/2}$. Since $\Gamma \approx 0.6$ MeV, $E_c \approx 1$ MeV, and $E_s \approx 83$ MeV for 90 MeV incident α particles, we see that the angular correlation between the α particle and neutron is blurred by 4° from this effect alone.

IV. RESULTS

A. Confirmation of the production of ⁵He

The results obtained in each run were plotted as numbers of events per unit area in E_n vs E_α space. It was decided to use these two variables rather than the more directly observed variables E_α and neutron time of flight in order to treat both neutron

and α particle in similar, easily interpretable terms. One must remember, when looking at distributions in E_n - E_α space that, although the precision of E_α determination is more or less uniform throughout the plot, the precision of the E_n determination deteriorates rapidly as E_n increases.

A typical plot, that for 90 MeV α 's on ²⁰⁸Pb, with the α and neutron counters virtually coaligned ($\theta_n = 20^\circ$, $\theta_\alpha = 22^\circ$), is shown in Fig. 2. In preparing this figure a rather small number of accidental events was subtracted. These were measured by studying the coincidences which occur when the α -neutron time difference is shifted by one cyclotron period from the normal running conditions. The solid line in the figure corresponds to $E_\alpha + E_n = 81.3$ MeV. This is the maximum kinematically allowed energy for this sum. It corresponds to leaving the residual ²⁰⁷Pb in its ground state. One sees that, except in the immediate neighborhood of the solid line, there are no events to speak of in the kinematically disallowed region. There is some spilling of allowed events over the line due mainly to poor neutron energy resolution. Note, as we have mentioned above, that this resolution is worse at higher neutron energies.

The most striking topographical feature of our plot is the presence of the two hills more or less centered on the kinematic limit line. We ascribe these hills to (α , ⁵He (g.s.)) events where the ⁵He breakup direction coincides with the flight direction. The concentric curves drawn around the hills are counting-rate contours whose spacing is 5 counts per unit area.

To establish whether the hills come from the (α , ⁵He) process, one can compare their properties to those expected for the collinear counter geometry (see Fig. 1). According to Eq. (2a) the average of the two α particle energies observable in this geometry should be $\frac{1}{5}(4E_s + E_c)$, and the difference should be $\frac{3}{5}(E_s E_c)^{1/2}$. Now, E_c for the ⁵He ground state is 0.89 MeV¹¹ and the maximum possible value of E_s is 81.3 MeV.¹² (We are assuming here that the ²⁰⁷Pb is left in its ground state and are taking into account a 0.4 MeV energy loss in the Pb target.) These values give 65.2 and 13.6 MeV for the average and difference α particle energies, respectively. Now, the observed centroids of the two hills have α particle energies of 59.8 and 72.7 MeV. The average of these energies is 66.2 MeV and the difference is 12.9 MeV. Although these values are both within 1 MeV of the expected values, the observed average energy is actually a bit too high for comfort. Had we assumed the average residual excitation energy in the ²⁰⁷Pb to be ~ 1 MeV (as it seems to be—see Sec. IV B) rather than 0 MeV, our expected average α particle energy would have

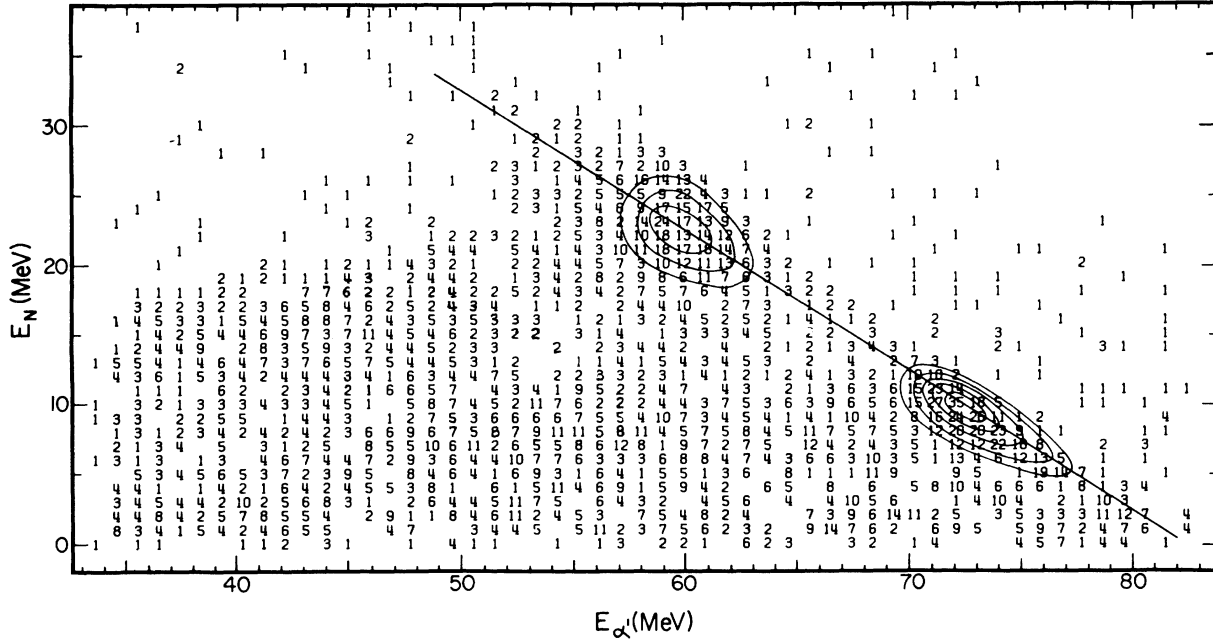


FIG. 2. The α - n coincidence spectrum from ^{208}Pb bombarded with 90 MeV α particles. The α counter was at 22° and the neutron counter was at 20° . The total integrated charge was $52.2 \mu\text{C}$. To express these results in units of $\mu\text{b}/\text{MeV}^2 \text{sr}^2$ the numbers of counts shown throughout the plot should be multiplied by 4.90 and divided by the appropriate neutron detector efficiency. The diagonal line gives the kinematic limit. It corresponds to events which leave the ^{207}Pb unexcited. The contours mark the clusters of events characteristic of the formation and breakup of ^5He which leave the ^{207}Pb in some very low-lying state.

dropped to 64.4 MeV, even further (1.8 MeV) below the observed value.

This discrepancy can be accounted for, within the uncertainties of measurement, if we take the short half-life of the ^5He ground state into account. From the width of this state and the ^5He kinetic energy, one can deduce that about half the ^5He 's decay within ~ 40 fm of the target nucleus, and about half decay at greater distances. The Coulomb potential energy between Pb and ^5He at this median distance is about 6 MeV. If the ^5He manages to leave the Coulomb field before breakup (as was tacitly assumed in the discussion of ^5He breakup kinematics in Sec. II), the α particle receives on the average $\frac{4}{5}$ of the Coulomb potential energy of the ^5He at 40 fm, namely $\frac{4}{5} \times 6$ MeV, but if the breakup occurs at 40 fm, the α particle receives instead the full 6 MeV upon emerging from the Coulomb field. Since 40 fm is the median breakup location, the α particles should have an average energy $\sim \frac{6}{5}$ MeV larger than our earlier considerations would have led us to expect. The exponential distribution of decay times should warp the shape of both hills by stretching them in the direction of higher α particle energy. This effect seems to be visible in the data. In short, both the location and shapes of the hills on the E_α - E_n plane are in good quantitative accord with the as-

sumption that they arise from the $(\alpha, ^5\text{He} \text{ (g.s.)})$ reaction.

Even when neutron and α counters are not placed at the same angle to the beam, as long as the angle between them remains small enough [see Eq. (1)], the ^5He breakups will produce two hills in the E_α - E_n plane. As the angle between counters increases these hills move toward each other until, finally, when the kinematic limiting angle is reached, the hills have merged. As the hills move toward each other they broaden since, at the limit, a small spread in breakup angle translates into a sizable spread in particle energies. This motion and broadening of the hills appears clearly in our data and is shown in Fig. 3, where the contours in the hill regions have been traced from plots like those in Fig. 2. For angular separations between the counters larger than those to which ^5He 's could be expected to contribute, no hills appear in the data.

A further kinematic check (independent of the foregoing ones) of the interpretation that the hills arise from ^5He breakup is provided by the ratio of total counts under the two hills. We have seen [Eq. (4)] that for the coaligned geometry the ratio of the numbers of particle pairs entering both detectors for the higher to lower energy α particle groups is $(E_\alpha^F E_n^B)/(E_\alpha^B E_n^F)$, i.e., it is equal to the

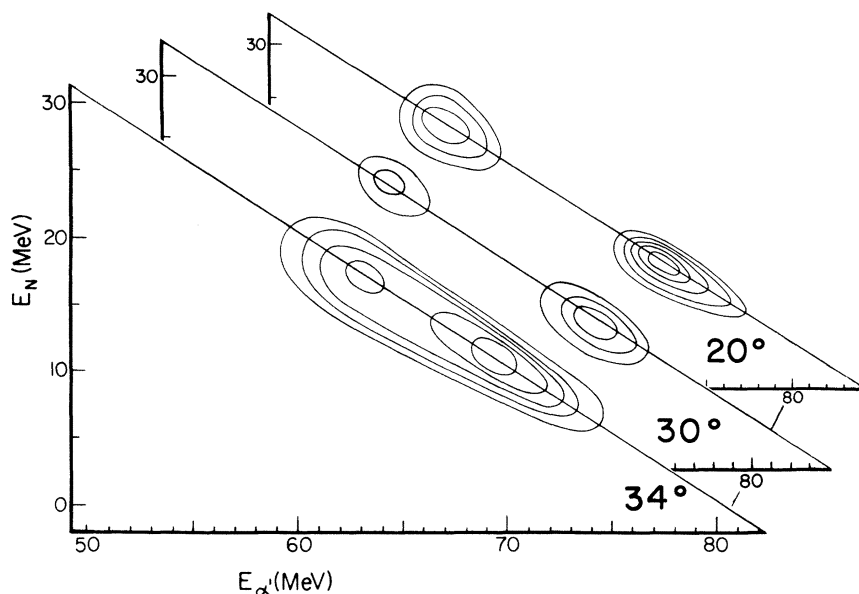


FIG. 3. The intensity contours in the neighborhood of the peaks in the α - n coincidence spectra from the $(\alpha, {}^5\text{He}(g.s.))$ reaction. These spectra were taken with the α counter at 22° and the neutron counter at the indicated angles. They were traced from figures like Fig. 2 and show clearly how the separation of the ${}^5\text{He}$ peaks decreases gradually from the value observed with coaligned counters—until the peaks merge, when the angle between counters is the largest possible consistent with the kinematics of the ${}^5\text{He}$ breakup. This behavior of the observed peaks is one of the clearest kinematic signatures for the ${}^5\text{He}$ reaction. (It should be noted that the incident energy in the 34° run was 2 MeV below that in the other two runs.)

ratio of the products of the particle energies in each of the two groups. For the 90 MeV bombardment this ratio has the value 0.48. (Note that the ratio of forward to back neutron energies is much greater than that for the α particles). To obtain the overall detection efficiency ratio, this geometric efficiency ratio must be multiplied by the intrinsic efficiency ratio in the neutron detector. For the average energy neutrons in each group, this ratio is 1.85. (The chance for an interaction in the neutron detector is significantly larger for the lower energy neutrons than for the higher energy group.) Thus the expected counting rate ratio for the two ${}^5\text{He}$ peaks is $0.48 \times 1.85 = 0.88$. The corresponding measured ratio is observed to be 0.90 ± 0.06 . This seems to be in adequate accord with expectations. (In estimating the expected ratio, we have neglected some small corrections arising from Coulomb effects on the trajectories.)

B. Special features of the $(\alpha, {}^5\text{He})$ reaction

Having shown that events coming from ground state ${}^5\text{He}$ breakups can straightforwardly and consistently be distinguished from other events which lead to α - n coincidences, it is reasonable to ask what have we managed to learn about the $(\alpha, {}^5\text{He}(g.s.))$ reaction. We take up in turn the magnitudes of the cross sections, the spectrum of residual excitations in the target nucleus, and the

angular distributions of the outgoing particles.

To determine $(\alpha, {}^5\text{He})$ differential cross sections from our observations of the α, n coincidence pattern in a particular counter configuration, one must assume some form for the c.m. ${}^5\text{He}$ breakup angular distribution. We take this distribution to be isotropic. At a mean angle for emitted ${}^5\text{He}$'s of 22° the differential cross section for their emission in a 90 MeV α particle bombardment of ${}^{208}\text{Pb}$ was found to be 25.6 ± 3.1 mb/sr. It should be pointed out that the ${}^5\text{He}$ directions being sampled in any placement of the α and neutron detectors are distributed over an angular interval approximated by the angular width of the α particle counter (typically around 5°). The quoted cross sections are averages over such intervals. Table I lists some of the differential cross sections that were measured at 90 and at 42 MeV. For the targets other than Pb, the runs were always taken with neutron and α particle counters at a common angle. It had been found that this arrangement gives the cleanest signature for ${}^5\text{He}(g.s.)$ events. It is, of course, necessary in this counter arrangement to make a (small) correction for the absorption of neutrons in the α particle detector. It is seen from the table that the $(\alpha, {}^5\text{He}(g.s.))$ cross section is a substantial cross section, comparable with pickup cross sections which lead to bound residual states.¹³

TABLE I. Differential cross sections for the $(\alpha, {}^5\text{He}(\text{g.s.}))$ reaction.

Target	Incident α energy (MeV)	${}^5\text{He}(\text{g.s.})$ lab angle (deg)	Cross section to low-lying residual states ^a (mb/sr)
${}^{208}\text{Pb}$	42	30	21 ± 6.0
	42	45	6.5 ± 1.7
	90	22	25.6 ± 3.1
	90	26.5	11.0 ± 1.9
C	90	21.5	6.1 ± 1.0
Rh	90	21.5	5.5 ± 3.0
U	90	21.5	19.7 ± 5.1

^a These states span the lowest 3 MeV of excitation.

It may help in considering the trend with target mass number of the cross sections in Table I to look at the counting rate contours in the $E_n - E_\alpha$ plane for our four targets (Fig. 4). The Q value for the $(\alpha, {}^5\text{He}(\text{g.s.}))$ reaction in carbon is considerably lower than it is for the other three nuclei. This accounts for the fact that the value of $E_n + E_\alpha$ through the center of the hills in carbon is visibly smaller than it is for the other targets. The separations between hills are more nearly the same for all targets because the Q value has less bearing on the separation than it does on the average energy of the hill centroids.

The carbon hills are also significantly sharper

than the others. With targets as light as carbon the broadening of the hills due to Coulomb effects on the breakup energies is rather negligible.

The elongated shape of the rhodium hills reflects the fact that the residual ${}^{102}\text{Rh}$ tends to be left in a broader range of excitations than the other targets. The $(\alpha, {}^5\text{He})$ reaction tends to favor small angular momentum transfer (see below), and in Rh the favored states are presumably at higher excitation. One should note that the direction of elongation of the hills due to the excitation of higher levels in the residual nucleus is *not* in a direction perpendicular to the lines $E_n + E_\alpha = \text{constant}$, but lean instead toward the $E_n = \text{constant}$ lines. This comes about because higher residual excitation corresponds to lower ${}^5\text{He}$ kinetic energy E_5 , and a reduction in E_5 has a much more telling effect on the α particle energy than it does on the neutron energy. [See, for example, Eq. (2)].

The favoring of low angular momentum transfers in the $(\alpha, {}^5\text{He}(\text{g.s.}))$ reaction at forward angles can be surmised from the small change in the mass-energy product of incoming and outgoing particles. For glancing trajectories the forward angular momentum transfer is classically less than $2\hbar$ for 90 MeV incident particles, and the results of DWBA calculations (Sec. V) are consistent with this low value. For example, the largest computed cross section occurs for the transfer of a $p_{3/2}$ neu-

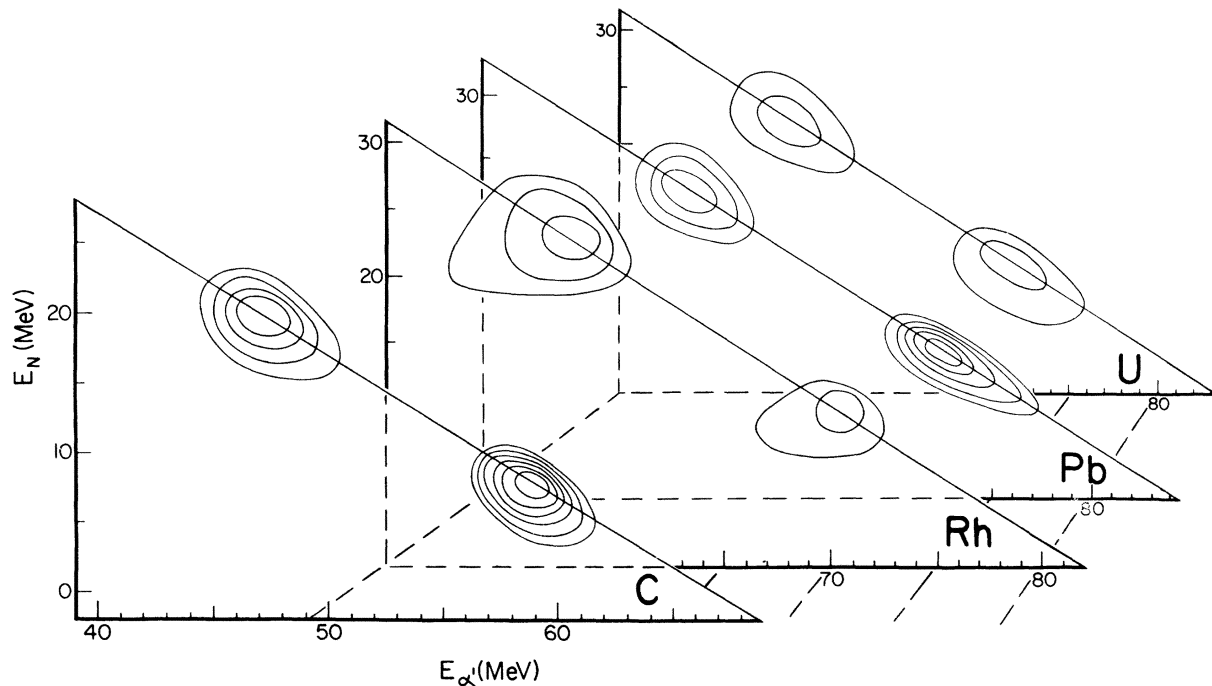


FIG. 4. The shapes of the α - n coincidence counting rate peaks for the $(\alpha, {}^5\text{He}(\text{g.s.}))$ reaction for different targets. In these runs the α and neutron counters were approximately collimated at $\sim 21.5^\circ$. The curves for carbon are shifted to lower n and α energies because of the large binding energy of neutrons to carbon.

tron. Unfortunately, we did not have the energy resolution in the neutron detector to properly separate yields to the various low-lying states in ^{207}Pb , but runs at both 42 MeV and at 90 MeV showed about twice as much yield to the three lowest ^{207}Pb levels ($p_{1/2}$ (g.s.), $f_{5/2}$ (0.57 MeV), and $p_{3/2}$ (0.90 MeV) as to the next three levels ($i_{13/2}$ (1.63 MeV), $f_{7/2}$ (2.34 MeV), and $h_{9/2}$ (3.43 MeV)).^{13,14}

The 90 MeV data were all obtained in a single running period of a few days at the Berkeley cyclotron and we were consequently able to only touch upon many of the features of the (α , ^5He) reaction. For example, the (α , ^5He) differential cross sections for our major target ^{208}Pb were measured at only two angles (Table I). This hardly constitutes an angular distribution. It is therefore comforting to find (Fig. 5) that very slight extrapolations in angle of the present data are in good agreement with the differential cross sections obtained by Chenevert¹⁰ for the mesa in the (α , α') spectra he observed at 90 MeV. Chenevert took data at 5° intervals in the forward directions and found a smooth angular distribution for the mesa. DWBA calculations (Sec. V) show that a smooth distribution is expected for the (α , ^5He) process at these energies.

In addition to the question of the angular distri-

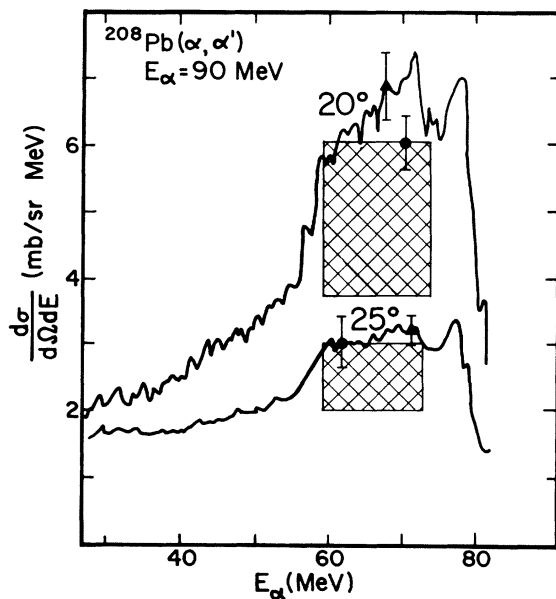


FIG. 5. The cross-hatched areas give the contributions to the α' spectra seen in a one counter experiment due to ^5He (g.s.) production as determined in the present experiment. The curves are the measured (α , α') spectra of Chenevert (Refs. 1, 10). It is seen that the highest energy part of the mesa in the (α , α') spectra is not accounted for by ^5He production. It is in part due to the excitation of the $E2$ giant resonance (Ref. 15).

bution of the emitted ^5He (g.s.) with respect to the c.m. of the large system, α + target nucleus, there is the interesting matter of the angular distribution of the breakup products α and neutron in the c.m. system of the ^5He . The ^5He ground state is a $p_{3/2}$ state and the most general form of the breakup angular distribution would therefore be $a_0 + a_2 P_2(\cos\theta)$, where θ is the angle between the breakup direction and an appropriate symmetry axis. In a plane wave Born approximation, it is easy to appreciate that this symmetry direction is along the relative velocity of the incident α particle and the neutron to be picked up, i.e., along the direction of the α particle velocity in the ^5He c.m. system. In fact, in plane wave Born approximation (PWBA) the breakup angular distribution happens to be¹⁶ simply $1 + P_2(\cos\theta)$. The symmetry axis for breakup lies in the scattering plane but it is *not* along the ^5He flight direction. This feature holds as well in models more realistic than the PWBA. It implies that with any arrangement of counters (other than the collinear one) the two hills seen for ^5He breakup need not be of equal intensity since they correspond to *different* c.m. breakup angles θ with respect to the symmetry axis. In principle, measurements of the two-dimensional α - n coincidence spectra would provide information about the c.m. breakup angular distribution and hence about the polarization state of the ^5He . This would be very useful information to have in any study of the details of the pickup mechanism. The precision of the present measurements was unfortunately not quite up to the extraction of such information. It has been indicated, in this connection, that in estimating ^5He production cross sections from measurements with the collinear detector geometry it was assumed that the c.m. breakup intensity in the ^5He flight direction was equal to the average intensity over all directions. This may not be a valid assumption and the cross sections in Table I may be in error on this score by as much as 20%.

C. Coincidence events other than those involving ^5He (g.s.)

It is seen from Fig. 2 that there are many α - n coincident events in addition to those we have attributed to the pickup reaction leading to ^5He (g.s.). The number of such events is larger the more forward the α and neutron counters are and becomes very small for large angular separations between the counters. These observations suggest that we are looking at coincident products of direct reactions and that some of these products arise from the breakup of short-lived intermediate states. There is, of course, no reason to believe that ^5He will be produced only in its ground state.

The higher states are much wider than the ground state and do not give such crisp kinematic signatures, nor is their production uniquely describable as a pickup. As the states broaden compared with their spacing, the distinction between pickup and knock-on direct reactions blurs. It would nonetheless be of interest to study further than we have been able to do here the yields of coincident products to unbound states precisely to see which reaction mechanism formulations best describe the results.

We must call attention to one unexpected observation in the coincidence spectra. In Fig. 6 we can see two clusters of high intensity in the regions ringed by dashed curves. The missing energy associated with these clusters is of the order of 20 MeV. That is, either the residual nucleus or other reaction products must be taking up this large amount of energy. It is easy to establish that the 20 MeV is not simply excitation energy of some especially excitable states in ^{207}Pb . The location of the bumps simply does not correspond to the kinematic requirements for the production of $^5\text{He(g.s.)}$ along with an excited state in ^{207}Pb .

After some thought, it was realized that these

clusters arise from the reaction $(\alpha, ^6\text{He}^*)$, where the $^6\text{He}^*$ is made in its 2^* state at 1.8 MeV, and that this state decays to $^5\text{He(g.s.)} + n$ with $^5\text{He(g.s.)}$ subsequently decaying to $\alpha + n$. The unexpected feature here is that there would be a concentration in the phase space of a single pair of particles (α and n) when there are *four* particles in the final state. Even when there are only three particles in the final state [e.g., in $(\alpha, ^5\text{He(g.s.)})$], one does not get easily observable correlations unless the intermediate state responsible for these correlations is rather narrow. By chance the two intermediate states in $(\alpha, ^6\text{He}^*)$ are narrow enough. The 1.8 MeV state in ^6He is only 0.11 MeV wide¹¹ and the effective width of the ^5He ground state is, in this case, narrower than its actual width of 0.6 MeV. Although the decay sequence of $^6\text{He}^*$ (1.8) has not been measured we can deduce from general considerations what this sequence should be. The $^6\text{He}^*$ decays by emitting one *p*-wave neutron instead of a *d*-wave dineutron because the former emission is favored by a more penetrable centrifugal barrier, but even in the one-neutron emission, the barrier has the effect to make the neutron come out with a c.m. energy not much less than 0.4 MeV.

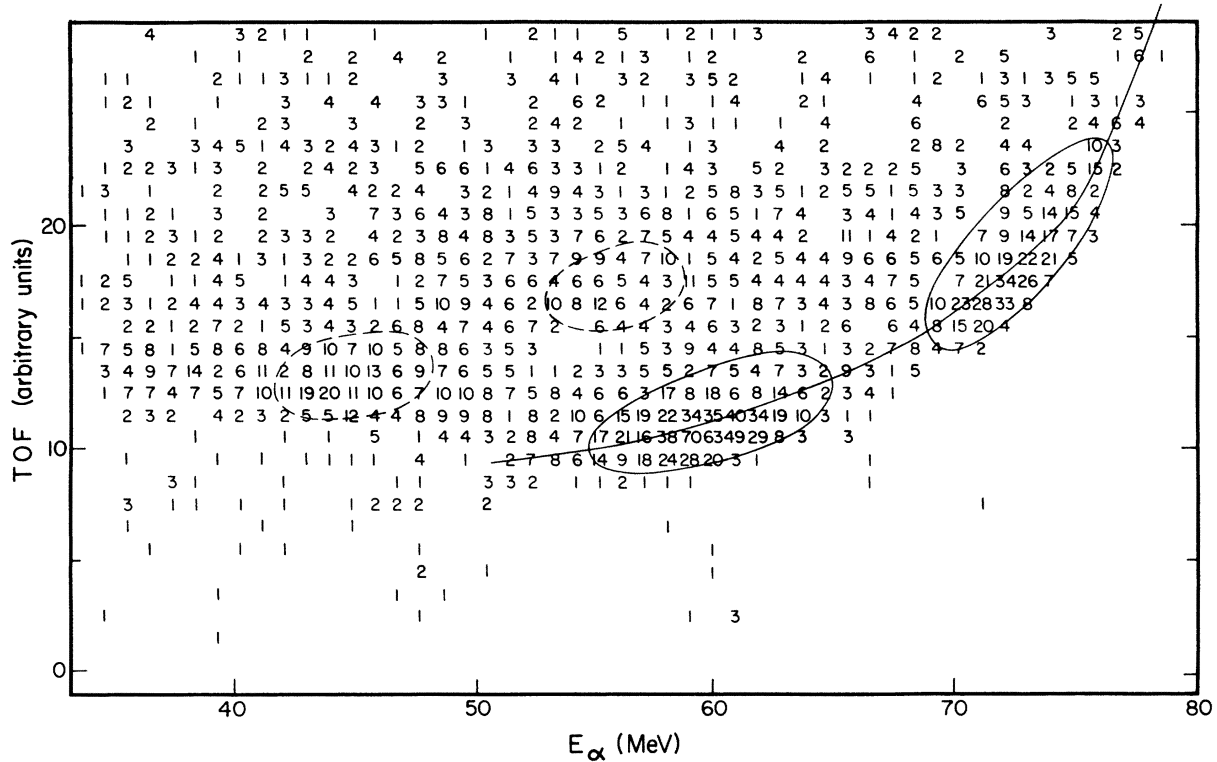


FIG. 6. The spectrum of α - n coincidence events with a ^{208}Pb target, 90 MeV incident α particles, and the α and neutron detectors at 22° and 20° , respectively. (The same conditions as in Fig. 2). When the neutron data are plotted in terms of time of flight as actually measured, it is easier to discern the unexpected clusters (dashed rings) than it is when the data are replotted in terms of neutron energy. These clusters are interpreted to represent events arising from the decay of ^6He (1.8 MeV) which is produced as a pickup product.

This leaves the ${}^5\text{He}(\text{g.s.})$ at an excitation of only 0.5 MeV, about half the centroid energy for this state. The centrifugal barrier in the subsequent p -wave decay of the ${}^5\text{He}$ narrows the options for energy division between the final α particle and neutron.

We can appreciate what we must expect from this sequence of decays in terms of what we already know about the kinematics of the ${}^5\text{He}(\text{g.s.})$ decay. The ${}^6\text{He}^*$ decays to ${}^5\text{He}(\text{g.s.})$ nuclei which move very nearly in the original ${}^6\text{He}^*$ direction and which have a uniform kinetic energy distribution of width $4 \times E_{\text{g}}^{1/2} E_{\text{c}}^{*1/2}$. Here E_{g} is the ${}^5\text{He}$ particle's share of the kinetic energy of the ${}^6\text{He}^*$, say 60 MeV for 90 MeV incident α particles, and E_{c}^* is the ${}^5\text{He}(\text{g.s.})$ share of the breakup energy of the ${}^6\text{He}^*$. E_{c}^* would be about 0.07 MeV. With these values the emitted ${}^5\text{He}(\text{g.s.})$ nuclei have a kinetic energy spread of about 8 MeV and an average energy of about 60 MeV. Thus the decays of ${}^6\text{He}^*(1.8)$ give rise to a set of ${}^5\text{He}(\text{g.s.})$ particles that differ from those appearing directly in that they have a somewhat greater spread in kinetic energy and a somewhat lesser spread in internal energy. We have seen (e.g., in the discussion of the count rate pattern for the Rh target) that even when the ${}^5\text{He}(\text{g.s.})$ does have a broad kinetic energy spread one still sees the same characteristic hills in the coaligned geometry. They merely become broadened in a direction almost parallel to the α particle energy axis. We can therefore understand the appearance of two broad clusters in the coincidence plots which come from the production of ${}^6\text{He}^*(1.8)$ particles. A more detailed examination of the decays¹⁷ confirms that the observed clusters are where they should be for the production and decay of these particles and permits a rough estimate of the magnitude of the $(\alpha, {}^6\text{He}^*(1.8))$ differential cross section at 22° . It is 1 ± 0.25 mb/sr from ${}^{208}\text{Pb}$, about the same for ${}^{\text{nat}}\text{U}$, and only half as large for ${}^{103}\text{Rh}$. We cannot estimate the cross section for carbon because some of the relevant α particle energies in this case fall below the detector threshold.

The observation of ${}^6\text{He}^*(1.8)$ suggests of course that there must be pickup to higher states of ${}^6\text{He}$, too, but that we cannot distinguish their decay products because they are too broadly spread about in the E_{α} - E_n plane. One can also imagine that even heavier helium isotopes than ${}^6\text{He}$ may contribute to the correlated α - n spectra which we have observed.

V. DWBA CALCULATION OF THE $(\alpha, {}^5\text{He}(\text{g.s.}))$ DIFFERENTIAL CROSS SECTION

Pong and Austern¹⁶ as well as Ho and Henley¹⁸ have carried out DWBA calculations of the pickup

of $3p_{1/2}$ neutrons from ${}^{208}\text{Pb}$ by α particles. The magnitudes of the calculated cross sections were about the right size to explain the cross section of the mesa in the (α, α') spectra observed by Chenevert *et al.* We have extended these earlier calculations to additional angular momentum states using, this time, full-recoil exact finite-range codes^{19,20} in which the form of the internal ${}^5\text{He}$ wave function was that of an (unbound) scattering state. The formalism used was the one developed by Vincent and Fortune³ for stripping (rather than pickup) to unbound states. In the pickup calculations the short range of the α - n interaction limits the range needed for the radial integrals despite the unbound nature of the ${}^5\text{He}$. The differential cross section for pickup in this formalism is

$$\frac{d\sigma}{d\Omega} = \frac{2}{\pi\hbar^2} \mu_{\alpha n} \int dE_{\alpha n} k_{\alpha n} \frac{d\sigma^F}{d\Omega}, \quad (5)$$

where the cross sections $d\sigma^F/d\Omega$ are defined in terms of the T matrix just as they are for bound states, although here the internal ${}^5\text{He}$ wave function cannot be normalized as a bound state can, and is instead normalized to unit amplitude at large distance. (The superscript F is the Vincent-Fortune notation for this fictitious cross section.) Enough is known about the α - n system²¹ in the relevant energy range to make the integration over $E_{\alpha n}$ straightforward. Details are given elsewhere.¹⁷

Since only with ${}^{208}\text{Pb}$ had we measured $(d\sigma/d\Omega)(\alpha, {}^5\text{He})$ at more than one angle, it was decided to limit the calculation of $d\sigma/d\Omega$ to this one target. The optical model parameters that were used are displayed in Table II. Note that the parameters for ${}^5\text{He}$ were assumed to be the same as those for an α particle. The results are given in Fig. 7 for different single-particle states in the residual ${}^{207}\text{Pb}$. (Preliminary calculations with zero range DWBA showed the contribution from the higher l states $i_{13/2}$ and $h_{9/2}$ to be small, and consequently they were not included in our finite-range full-recoil calculations.) The experimental points refer to the summed yields to all low-lying states in ${}^{207}\text{Pb}$, since we were unable to resolve these states individually. These are the f and p states and the calculated sum of their yields is the heavy line labeled "sum". It is seen that, as expected, the reaction favors the lowest l 's. It also appears that the calculations are in reasonable agreement with experiment both as to magnitude and as to rate of change with angle. It should be remarked that not unreasonable changes in the ${}^5\text{He}$ optical model parameters can vary the magnitude of the cross section by as much as 50%; such changes do not, however, seem to affect the slope of the differential cross section. In short, the DWBA, suitably modified to cope with a projectile in an unbound state,

TABLE II. Optical model parameters used in DWBA calculation of $(\alpha, {}^5\text{He}(\text{g.s.}))$ cross section on ${}^{208}\text{Pb}$.

System	V (MeV)	r_0 (fm)	a (fm)	W (MeV)	r_i (fm)	d_i (fm)	V_{so} (MeV)
${}^{207}\text{Pb}-n$	45.53	1.25	0.65				7.0
${}^{208}\text{Pb}-\alpha^a$	84.12	1.387	0.660	36.61	1.42	1.387	
${}^{207}\text{Pb}-{}^5\text{He}$	84.12	1.387	0.660	36.61	1.42	1.387	
${}^4\text{He}-n^b$	41.90	1.488	0.25				13.441

^a Deduced from fit to elastic scattering differential cross sections at 96 MeV measured at Texas A & M Cyclotron.

^b From Ref. 21.

seems to do reasonably well in accounting for the measured $(\alpha, {}^5\text{He}(\text{g.s.}))$ cross section in ${}^{208}\text{Pb}$.

VI. DISCUSSION AND CONCLUSIONS

We have found the differential cross section for the $(\alpha, {}^5\text{He}(\text{g.s.}))$ reaction on medium and heavy targets (≥ 10 mb/sr) to be comparable to those for pickup reactions where the emerging particle is bound. The breakup of the ${}^5\text{He}$ casts the α particle into the inelastic spectrum producing there a bump-like structure of magnitude ~ 1 mb/(sr MeV) for forward directions. We have also observed the pickup of two neutrons to produce excited ${}^6\text{He}^*(1.8)$ MeV) particles with differential cross sections at forward angles about one order of magnitude smaller than that for ${}^5\text{He}(\text{g.s.})$. The ${}^6\text{He}^*(1.8)$ nuclei decay sequentially to ${}^5\text{He}+n-\alpha+n+n$. There are too few of these decays to give a noticeable effect in the inelastic spectrum. In addition to the events proceeding through ${}^5\text{He}(\text{g.s.})$ and ${}^6\text{He}^*(1.8)$, there are a large number of correlated α - n coincidences for which we could not identify a well defined intermediate state. These coincident particles come off in forward directions and the cross section for their emission increases as the angle between α particle and neutron decreases. We have not studied these coincidence spectra at enough pairs of angles to characterize them more sharply nor to estimate their total cross section with any precision.

The ${}^5\text{He}(\text{g.s.})$ yields and angular distributions were found to be in reasonable accord with theoretical expectations. The comparisons with theory could be sharpened up if one were to resolve the levels in the heavy residual nucleus better than we were able to. If this were done, it would be interesting to determine the polarization state of the ${}^5\text{He}$ by measuring its center-of-mass breakup angular distribution.

ACKNOWLEDGMENTS

We gratefully acknowledge the assistance of Dr. R. Heffner, K.-L. Liu, and W. Trautmann

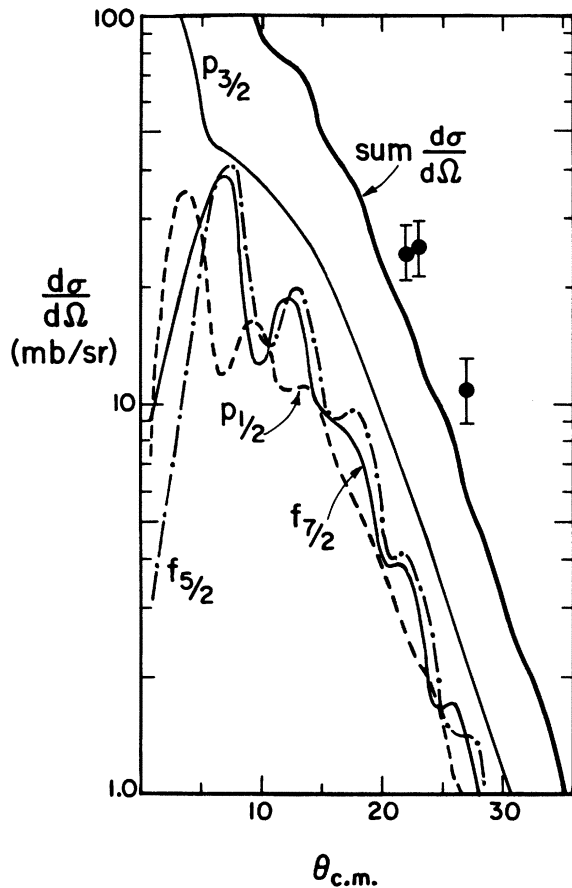


FIG. 7. Calculated and measured differential cross sections for the $(\alpha, {}^5\text{He}(\text{g.s.}))$ reaction on ${}^{208}\text{Pb}$. The curve labeled sum gives the total calculated cross section to the p and f hole states in ${}^{207}\text{Pb}$. (The individual cross sections to these states are also plotted.) The data points were obtained in the present experiment and correspond to the sum over residual excitations to about 3 MeV.

during some of these experiments. We would like to thank Professor H. Morinaga for suggesting the possible contribution of the α , ^5He reaction to inclusive α , α' spectra, and Dr. R. M. DeVries for his help in carrying out the finite-range DWBA

calculations. For their continued interest and many helpful discussions we must thank Professor N. Austern, Dr. W. S. Pong, Dr. H. W. Ho, Professor E. M. Henley, and Professor J. S. Blair.

*Work supported in part by U.S. Energy Research and Development Administration.

† Present address: Cyclotron Institute, Texas A & M University, College Station, Texas.

‡ Present address: Varian Physics Laboratory, Stanford University, Stanford, California.

§ Present address: Lawrence Berkeley Laboratory, University of California, Berkeley, California.

|| Permanent address: Hahn-Meitner Institute, Berlin, West Germany.

¹G. M. Chenevert, N. S. Chant, I. Halpern, C. Glashauser, and D. L. Hendrie, *Phys. Rev. Lett.* **27**, 434 (1971).

²D. H. Youngblood, R. L. Kozub, R. A. Kenefick, and J. C. Hiebert, *Phys. Rev. C* **2**, 477 (1970).

³C. M. Vincent and H. T. Fortune, *Phys. Rev. C* **2**, 782 (1970).

⁴B. L. Cohen, E. C. May, T. M. O'Keefe, and C. L. Fink, *Phys. Rev.* **179**, 962 (1969).

⁵R. E. Brown, J. S. Blair, D. Bodansky, N. Cue, and C. K. Kavaloski, *Phys. Rev.* **138**, B1394 (1965).

⁶See, e.g., G. C. Phillips, *Rev. Mod. Phys.* **37**, 409 (1965), and other papers in this volume.

⁷D. R. Brown, I. Halpern, K.-L. Liu, P. A. Russo, and W. Trautmann, *Nuclear Physics Laboratory Annual Report*, University of Washington, 1972 (unpublished), p. 81.

⁸D. R. Brown, I. Halpern, R. Heffner, K.-L. Liu, and P. Russo, *Bull. Am. Phys. Soc.* **17**, 927 (1972); D. R. Brown, I. Halpern, D. L. Hendrie, and H. Homeyer,

Bull. Am. Phys. Soc. **19**, 507 (1974).

⁹C. Pirart, M. Bosman, P. Leleux, P. C. Macq, and J. P. Meulders, *Phys. Rev. C* **10**, 651 (1974).

¹⁰G. M. Chenevert, Ph.D. thesis, University of Washington, 1969 (unpublished).

¹¹F. Ajzenberg-Selove and T. Lauritsen, *Nucl. Phys.* **A227**, 1 (1974).

¹²C. Maples, G. W. Goth, and J. Cerny, UCRL Report No. 16964, 1966 (unpublished).

¹³See e.g., W. C. Parkinson, D. L. Hendrie, H. H. Duhn, J. Mahoney, J. Saundinos, and G. R. Satchler, *Phys. Rev.* **178**, 1976 (1969).

¹⁴C. M. Lederer, J. M. Hollander, and I. Perlman, *Table of Isotopes* (Wiley, New York, 1968), 6th Ed.

¹⁵D. H. Youngblood, J. M. Moss, C. M. Rozsa, J. D. Bronson, A. D. Bacher, and D. R. Brown, *Phys. Rev. C* (to be published).

¹⁶W. S. Pong and N. Austern, *Nucl. Phys.* **A221**, 221 (1974).

¹⁷D. R. Brown, Ph.D. thesis, University of Washington, 1974 (unpublished).

¹⁸H. W. Ho and E. M. Henley, *Nucl. Phys.* **A225**, 205 (1974).

¹⁹R. M. DeVries, Finite Range Code LOLA (private communication).

²⁰T. Tamura and K. S. Low, *Comput. Phys. Commun.* **8**, 349 (1974).

²¹G. R. Satchler, L. W. Owen, A. J. Elwyn, G. L. Morgan, and R. C. Walter, *Nucl. Phys.* **A112**, 1 (1968).